



# Quantitative and qualitative analysis of the mass transfer and dispersion of methane injection under continuous mode shooting



Yeongseok Jang<sup>a,1</sup>, Jonghyun Oh<sup>b,1</sup>, Uendo Lee<sup>c</sup>, Jinmu Jung<sup>b,\*</sup>, Seuk-Cheun Choi<sup>c,\*</sup>

<sup>a</sup> Department of Mechanical Design Engineering, Chonbuk National University, Jeonju, Republic of Korea

<sup>b</sup> Department of Nano-bio Mechanical System Engineering, Chonbuk National University, Jeonju, Republic of Korea

<sup>c</sup> Thermochemical Energy System R&D Group, Korea Institute of Industrial Technology, Cheonan, Republic of Korea

## ARTICLE INFO

### Keywords:

Injection  
Methane  
Visualization  
Mass transfer  
Dispersion

## ABSTRACT

This study investigated the performance of a natural gas injector with regard to its mass transfer and fuel dispersion. A newly developed gas injector was fabricated with an injector nozzle size that was optimized based on computational fluid dynamics. High-speed injection images were analyzed with the injection parameters related to injection penetration length, injection cone angle, injection time, and injection area. Both  $\lambda$  (the ratio of mass per injection area) and  $J_p$  (a rate of change of pixel number to change of penetration length) were employed to estimate the quantity and quality of the dispersion. As a result, a uniform distribution and well-dispersed gas properties could be explained with low  $\lambda$  and high  $J_p$  values. The  $\lambda$  and  $J_p$  results could be a very useful index used to quantitatively and qualitatively evaluate the performance of natural gas injection.

© 2017 Published by Elsevier Ltd.

## 1. Introduction

The increased generation of particulates and harmful materials from a variety of sources has aggravated air pollution, resulting in global warming and an imbalanced ecosystem. Recently, this problem has been getting more serious due to an increased consumption of fossil fuels as the result of population growth and an improved quality of life [1–4]. Fossil fuel consumption especially generates nitrogen oxides, carbon dioxide, hydrocarbons, carbon monoxide and particulate matter to be potential threats to humans [1,5–7]. Therefore, many countries including developing countries have implemented advanced or enforced exhaust gas regulations and have installed gas monitoring systems to solve this problem [8–11]. To address the current issues, alternative fuels and optimized combustion systems have generated considerable interest.

Among the variety of available alternative fuels such as biomass and natural gas, natural gas is referred to as a clean fuel, consisting of at least 90% methane ( $\text{CH}_4$ ), ethane ( $\text{C}_2\text{H}_6$ ), propane ( $\text{C}_3\text{H}_8$ ), and butane ( $\text{C}_4\text{H}_{10}$ ) [2]. The characteristics of natural gas include a high octane number, high compressibility, and low carbon content. The aforementioned characteristics of natural gas within combustion systems can yield the following advantages. First, a high compressibility can enhance effective mass transfer during gas injection, resulting in a relatively high thermal efficiency compared to other liquid-based fuels [12–15]. Second, knock resistance (predetonation) during engine combustion can be

improved with a high octane number [2,16,17]. Third, the reduced carbon content within natural gas can reduce both  $\text{CO}_2$  emissions and particulate matter (PM) values compared to conventional engine emissions [18–21].

Within natural gas combustion systems, the injection behavior of gaseous fuel plays an important role with regard to improving engine performance. Therefore, many studies have focused on the characterization of injection parameters such as the injection penetration length, injection shape, injection angle, injector nozzle, and rail pressure. Delacout et al. [22] characterized high pressure diesel injection sprays using digital imaging techniques. Park et al. [23] analyzed injection spray penetration, spray area, and spray centroids using a visualization system. Yu et al. [24] investigated the flow structure and mixture formation of low pressure ratio wall-impinging jets using a natural gas injection system. Kim et al. [25] investigated the light intensity and image visualization of gasoline direct injection according to different nozzle hole locations. Park et al. [26] reported on fuel temperature dependent fuel flow and injection spray characteristics. Wang et al. [27] studied primary spray breakup at the initial injector opening stage during injection at atmospheric conditions.

In this study, we characterized the performance of a newly developed injector in order to achieve effective mass transfer and an enhanced dispersion of fuel. Based on computational fluid dynamics, an optimal injection nozzle size was determined. The optimized injector

\* Corresponding authors.

E-mail addresses: [jmjung@jbnu.ac.kr](mailto:jmjung@jbnu.ac.kr) (J. Jung), [chs30@kitech.re.kr](mailto:chs30@kitech.re.kr) (S.-C. Choi).

<sup>1</sup> Two authors were equally contributed to this article.

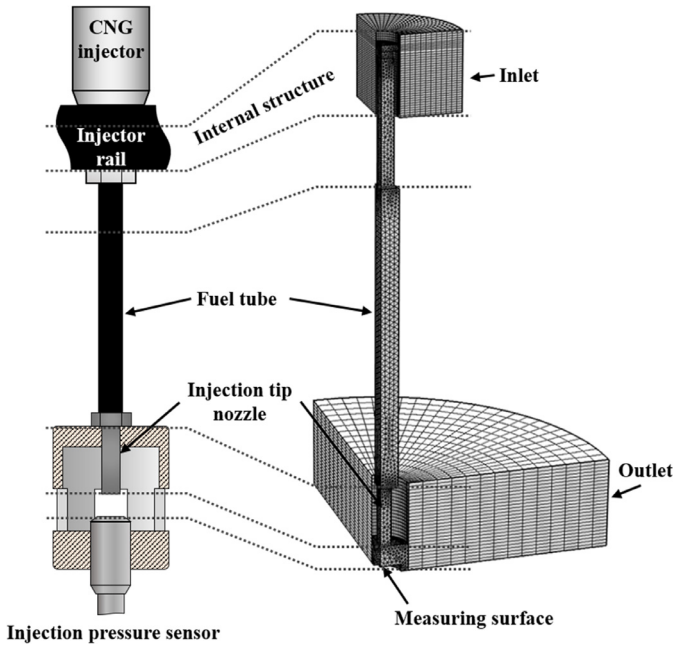


Fig. 1. Three-dimensional gas injector numerical model.

Table 1  
Properties of methane [29,30].

No.	Property	Unit	Value
1	Molecular weight	g/mol	16.043
2	Density	kg/m <sup>3</sup>	0.6797
3	Compressibility factor (Z)		0.99802
4	Heat of vaporization	kJ/kg	509.9
5	Lower heating value	kJ/kg	50.02 × 10 <sup>3</sup>
6	Higher heating value	kJ/kg	55.3 × 10 <sup>3</sup>
7	Diffusion coefficient in air	cm <sup>2</sup> /s	0.16
8	Autoignition temperature	K	813
9	Heat capacity at constant pressure (C <sub>p</sub> )	kJ/mol•K	0.0358
10	Heat capacity at constant volume (C <sub>v</sub> )	kJ/mol•K	0.0274
11	Ratio of specific heats (γ : $\frac{C_p}{C_v}$ ) @1.013 bar		1.3062
12	Viscosity	Pa•s	1.0245 × 10 <sup>-5</sup>
13	Thermal conductivity	mW/m•K	30.57

was fabricated via casting methods. Injection parameter characteristics were investigated using high-speed imaging analysis based on schlieren imaging methods.  $\lambda$  (the ratio of mass per injection area) and  $J_p$  (the pixel number change rate to the change in penetration length) were employed to analyze the quantity and quality of the dispersion.

## 2. Material and methods

### 2.1. CFD analysis

In order to determine the optimal nozzle size with regard to mass flow rate and injection pressure, a 3D geometry of the internal structure of the injector was prepared for computational fluid dynamics (CFD) analysis, as shown in Fig. 1. The gas used during the simulation was methane (CH<sub>4</sub>) because natural gas includes more than 90% methane (Table 1).

Pre-processing of the model was conducted. The injector inlet pressure was set to 120 kPa, 140 kPa, 160 kPa, and 180 kPa, respectively. The outlet pressure of the injector was set to atmospheric pressure. The following injector nozzle diameters were respectively considered: 1.5, 2.0, 2.5, 3.0, 3.5, 4.0, 4.5, 5.0, 5.5, 6.0, and 6.5 mm. The wall boundary function was considered under no-slip conditions.

In order to describe the mass transfer of methane, governing equations surrounding compressible flow (Ma < 0.3), RANS (Reynolds Aver-

aged Navier–Stokes) type, k-epsilon models were applied as follows:

$$\rho(\mathbf{u} \cdot \nabla)\mathbf{u} = \nabla \cdot [-p\mathbf{I} + (\mu + \mu_T)(\nabla\mathbf{u} + (\nabla\mathbf{u})^T) - \frac{2}{3}(\mu + \mu_T)(\nabla \cdot \mathbf{u})\mathbf{I} - \frac{2}{3}\rho k\mathbf{I}] + \mathbf{F} \quad (1)$$

$$\nabla \cdot (\rho\mathbf{u}) = 0 \quad (2)$$

$$\rho(\mathbf{u} \cdot \nabla)k = \nabla \cdot \left[ \left( \mu + \frac{\mu_T}{\sigma_k} \right) \nabla k \right] + P_k - \rho\epsilon \quad (3)$$

$$\rho(\mathbf{u} \cdot \nabla)\epsilon = \nabla \cdot \left[ \left( \mu + \frac{\mu_T}{\sigma_\epsilon} \right) \nabla \epsilon \right] + C_{\epsilon 1} \frac{\epsilon}{k} P_k - C_{\epsilon 2} \rho \frac{\epsilon^2}{k}, \quad \epsilon = \epsilon_p \quad (4)$$

$$\mu_T = \rho C_\mu \frac{k^2}{\epsilon} \quad (5)$$

$$P_k = \mu_T \left[ \nabla \mathbf{u} : (\nabla \mathbf{u} + (\nabla \mathbf{u})^T) - \frac{2}{3}(\nabla \cdot \mathbf{u})^2 \right] - \frac{2}{3}\rho k \nabla \cdot \mathbf{u} \quad (6)$$

where  $\rho$  is the density (kg/m<sup>3</sup>),  $\mathbf{u}$  is the velocity field (m/s),  $T$  is the temperature (K),  $p$  is the pressure (Pa),  $\mu$  is the dynamic viscosity (Pa•s),  $k$  is the turbulent kinetic energy (m<sup>2</sup>/s<sup>2</sup>),  $\epsilon$  is the turbulent dissipation rate (m<sup>2</sup>/s<sup>3</sup>), and  $C_{\epsilon 1}$ ,  $C_{\epsilon 2}$ ,  $C_\mu$ ,  $\sigma_k$ ,  $\sigma_\epsilon$ ,  $k_y$ , and  $B$  are interface parameters.

The geometry meshed with 50,000 tetrahedral elements was solved using the generalized minimal residual (GMRES) method. The injection pressure values of the simulated results were averaged from the obtained surface pressure profiles.

### 2.2. Fabrication of an injector

Based on the simulated results, an injector nozzle diameter of 3.5 mm was selected for the high mass transfer of methane. The newly designed injector consisted of four injection nozzles, four solenoid valves, and a fuel rail. Each part was fabricated with an aluminum casting. The coil body of the four solenoid valves was covered with heat-insulated plastic. The fabricated Peak and Hold injector operated at 12 V and 1.9  $\Omega$ .

### 2.3. High-speed imaging setup for injection visualization

Fig. 2 presents the high-speed imaging setup for injection visualization testing. Methane was used in the experiments as a replacement for natural gas. The injector inlet pressure for methane was regulated and monitored with a rail pressure sensor (4045A2, Kistler, Winterthur, Switzerland). In order to control mass transfer through the injector, methane injection was controlled by an electronic injector driver with a duty rate controller. The electronic signal from the driver was monitored with an oscilloscope (TDS-2024C, Tektronix, TX, USA). Acquired signals from the pressure sensor were stored by a data acquisition system (NI 9205, National Instrument, TX, USA). In order to investigate the mass transfer of methane, the rail pressure was measured under continuous mode operation by adjusting the inlet pressure between 120, 140, 160, and 180 kPa. The injector was set to open at 10 ms with a 70% duty rate in order to control the injection time.

Visualizations of methane injection were performed using schlieren photography methods. The experimental apparatus consisted of a laser light source, diffuser lens, aspherical lens, and a high-speed camera. The 532 nm laser light source possessed a power output of 15.0 mW (Edmund Optics Inc., NJ, USA), with a beam divergence of  $0.5 \pm 0.1$  mrad and a beam diameter of  $1.0 \pm 0.2$  mm. The modulation frequency of the laser was 10 kHz. Light from the laser travelled through two diffuser lenses and two symmetric aspherical lenses in order. Two diffuser lenses (9 & 18 mm and 20 & 50 mm in diameter & focal length) were used to expand the lights, and two symmetric aspherical lenses (150 & 450 mm in diameter & focal length) maintained a collimated beam. Methane injected from the nozzle located within the collimated beam was recorded using a high-speed camera (Fastcam SA3 model 120K-C1,

Download English Version:

<https://daneshyari.com/en/article/5015964>

Download Persian Version:

<https://daneshyari.com/article/5015964>

[Daneshyari.com](https://daneshyari.com)